Materials Advances

ROYAL SOCIETY OF CHEMISTRY

COMMUNICATION

View Article Online
View Journal | View Issue

Cite this: *Mater. Adv.*, 2024, 5, 1887

Received 19th October 2023,
Accepted 7th February 2024

DOI: 10.1039/d3ma00882g

rsc.li/materials-advances

Preparation of hydroxyapatite nanoparticle-hyaluronic acid hybrid membranes through citric acid molecular mediation†

Aoi Endo,[a] Zizhen Liu,[a] Daichi Noda,[ab] Mari Miyata[c] and Motohiro Tagaya *[a]

Citric acid (Cit)-coordinated hydroxyapatite (HAp) nanoparticles (NPs) were nanohybridized with hyaluronic acid (HYA) to form transparent membranes, where hydrogen bonds were formed between the NPs and HYA to change the hydration states. The interactions by the mediated Cit were found to be important for the nanohybridization between HAp and HYA.

It is well-known that biological hard tissues are naturally formed by nanohybrids of inorganic materials with polymers *in vivo*,[1,2] and the bonding states at the interfaces are important for the subsequent biological functions.[3,4] Mimicking the native interactive phenomena, nanohybrids of hydroxyapatite (HAp, $Ca_{10}(PO_4)_6(OH)_2$) with biopolymers have been widely studied *in vitro*.[5,6] In the hybridization process at the nanoscale, HAp is usually precipitated after fabricating the biopolymer membranes,[7,8] and the hybridization states are non-uniform because HAp is effectively deposited by recognizing the surface functional groups (*e.g.* –COOH groups, *etc.*)[9,10] of the biopolymer membranes without designing the interactive inner spaces. Thus, the initial hybridization states after dispersing the HAp nanoparticles (NPs) into the biopolymer solutions have been investigated.[11–13] However, there is a problem that the HAp NPs dramatically aggregate due to their higher surface free energy and induce the phase segregation between the HAp and biopolymer. From the above viewpoints, we suggested the importance of the design of the interactive network nanospaces between the HAp NPs and biopolymers inside the membrane, using hydrophilic biopolymers having the functional groups interacting with HAp NPs, leading to uniform nanohybridization. Collagen,[6,11,14] gelatin,[15,16] and alginate[17,18] are known as biopolymers that can easily interact with HAp NPs. If the spontaneously interactive nanospaces in the polymer network can be designed, we could achieve denser and more homogeneous HAp/biopolymer nanohybrids. In particular, hyaluronic acid (HYA) is a nontoxic and biocompatible polymer widely used in biomedical fields.[19–21] In the aqueous solution state, the –CONH and –COOH groups effectively approach each other through the hydrogen bonds mediated by water molecule coordination. Also, the hydrophobic region in the HYA is formed by 8 units of CH groups. Thus, HYA has a two-fold helix structure with a pitch length of 1.96 nm per turn.[22] The adjacent disaccharides are oriented in opposite directions to each other, and these phase-separated structures form network nanostructures in water with macroscopically twisted hydrophilic and hydrophobic groups.[23,24] The mesh size confined by the HYA molecular chains in the solution is about 10–100 nm. As an example, in a mixed solvent of 0.067 M phosphate buffer (pH = 7.3) and 0.179 M-NaCl, the mesh size of HYA has been measured by the fluorescence recovery after photobleaching technique of fluorescein isothiocyanate (FITC)-dextran,[25] where the mesh space matches the size of the calcium phosphate nucleus (*ca.* 30–100 nm)[26] and can be utilized as the nucleation site. Also, HYA has hydrophilic and bio-interactive functional groups such as –COOH, –OH, and –CONH.[23,24] Thus, studies to form calcium phosphate by diffusion and adsorption of Ca^{2+} and HPO_4^{2-} using the abundant functional groups of HYA have been reported.[27,28] Here, the pH in the solution changes the degree of ionization and deprotonation, which affects intra- and intermolecular interactions for forming the mesh structures.[29–31] Below the isoelectric point (pH = 2.5), the hydrogen bonds between the –CONH and –COOH groups result in close intermolecular distances. Above the isoelectric point, the deprotonation of the –COOH group leads to electrostatic repulsion among the $–COO^-$ groups, which makes it difficult to form the intermolecular hydrogen bonds, providing more 3-dimensional network polymer structures.[31,32] Based on the above background, when HYA forms swelled network structures in water under basic conditions, we hypothesized that the NPs

[a] *Department of Materials Science and Technology, Graduate School of Engineering, Nagaoka University of Technology, 1603-1 Kamitomioka, Nagaoka, Niigata 940-2188, Japan. E-mail: tagaya@mst.nagaokaut.ac.jp*
[b] *Research Fellow of the Japan Society for the Promotion of Science (DC), 5-3-1 Kojimachi, Chiyoda-ku, Tokyo 102-0083, Japan*
[c] *Department of Materials Engineering, National Institute of Technology, Nagaoka College, Nishikatakai 888, Nagaoka, Niigata 940-8532, Japan*

† Electronic supplementary information (ESI) available. See DOI: https://doi.org/10.1039/d3ma00882g

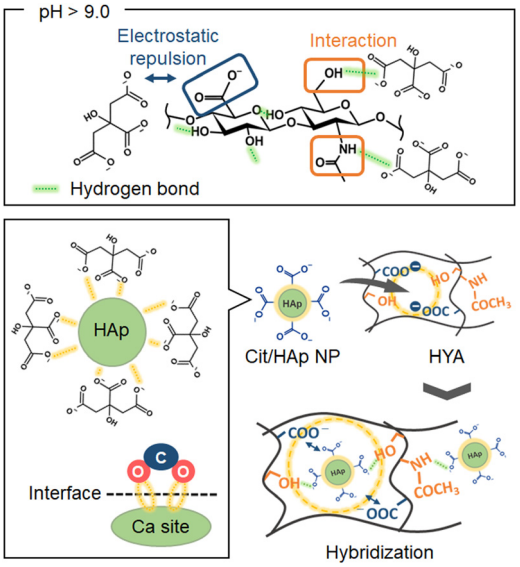

Scheme 1 Illustration of the preparation process for the hybrid membrane of the Cit/HAp NPs with HYA.

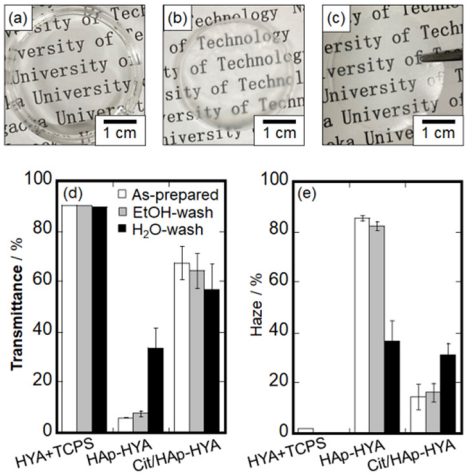

Fig. 1 Photographs of the as-prepared membranes of (a) HYA, (b) Hap-HYA and (c) Cit/HAp-HYA. (a) is difficult to peel from the TCPS dish and (b) and (c) can be picked up from the dish with tweezers. Optical (d) transmittance and (e) haze values of the membranes with the washing processes.

can diffuse into the mesh structures confined by the HYA molecular chains (*i.e.*, free spaces).

In this study, we aimed to prepare nanohybrid membranes of HAp NPs with HYA by utilizing the "free spaces" and functional groups of HYA as the immobilization region with the NPs (Scheme 1). In particular, we synthesized and used the HAp NPs coordinated with citric acid (Cit/HAp NPs).[33,34] Here, the aggregation among the NPs is inhibited by the electrostatic repulsion between the end $-COO^-$ groups of Cit.[33] Also, when the pH value is above 9.0, the Cit coordinated with HAp exists in a state where 3 protons have dissociated,[35] and can effectively interact with the $-CH_3OH$ and –CONH groups of HYA in the free spaces.[23] Thus, we suggested the introduction of Cit/HAp NPs into HYA, and the interactions with various functional groups of HYA were investigated to prepare the objective nanohybrids. In addition, the nanohybridization state (*i.e.*, HYA state in the membrane) was optimized by the solvent-washing process.

Sodium hyaluronate (HYA-Na, Mw: 850 000–1 600 000) was dissolved in ultrapure water at the concentration of 0.75 wt% and the solution was mixed with Cit/HAp NPs at the particle concentration of 1 wt% and stirred at 37 °C. Here, the NPs were synthesized according to our previous reports.[33,34] The final pH of the solution was adjusted to 9.0 with NaOH, and the solution was cast in a tissue culture polystyrene (TCPS) dish, and dried at 37 °C to obtain the membrane, which was named Cit/HAp-HYA. Then, the membrane was immersed in ethanol and immediately washed with ethanol or ultrapure water, and dried at 37 °C, named as Cit/HAp-HYA_X (X means the washing solvent (X = Et or Wa)). Based on the above procedure, membranes without NPs and membranes containing HAp NPs instead of Cit/HAp NPs were prepared and named HYA and HAp-HYA, respectively. All the membranes peeled from the TCPS dish, exhibiting self-standing and transparent properties, and were characterized by UV-visible photoabsorption spectrophotometer, X-ray diffraction (XRD), desktop-type scanning electron microscope (SEM), energy dispersive X-ray spectroscopy (EDS), X-ray fluorescence (XRF), atomic force microscope (AFM), Fourier transform infrared (FT-IR) spectrometer, and thermogravimetry-differential thermal analysis (TG-DTA). The evaluation methods of the transparency and hydration state are described in Experimental procedure S1, ESI.†

The photographs of the HYA, HAp-HYA, and Cit/HAp-HYA membranes and the results of the optical properties in terms of the transmittance and haze values are shown in Fig. 1. Photographs of the membranes washed with ethanol and water are shown in Fig. S1, ESI.† HYA was difficult to peel from TCPS (Fig. 1(a)), while HAp-HYA and Cit/HAp-HYA exhibited self-standing states after peeling from TCPS, especially HAp-HYA being turbid (Fig. 1(b) and (c)). When the optical property of HYA while adhering to TCPS was evaluated, high transparency was observed, with the transmittance of approximately 90% and the haze value of less than 2%. Although the transparency decreased with the inclusion of the NPs, Cit/HAp-HYA was more transparent than HAp-HYA. The transparency of the membrane is thought to be affected by the arrangement state of the NPs in the membrane, which would be attributed to the suppression of light scattering by the spherical shapes of the Cit/HAp NPs as compared with the case in the rod-shaped HAp NPs.[33] Furthermore, the Cit coordination caused electrostatic repulsion between the NPs,[33] which would also inhibit the NP aggregation to improve the transparency. Fig. S2, ESI† shows the XRD patterns of the HYA-Na and Cit/HAp NPs alone and the membranes. The Cit/HAp NPs were attributed to the HAp single phase (ICDD No.: 00-009-0432), and the HYA exhibited the amorphous state. In the membranes, there were diffraction peaks due to lower crystalline HAp or amorphous calcium phosphate.[36] The crystallite size in the (211) plane containing the Cit/HAp NPs was 16.3 nm for the powder, 9.6 nm for Cit/HAp-HYA, 13.6 nm for Cit/HAp-HYA_Et, and 10.9 nm for Cit/

HAp-HYA_Wa, indicating that the crystallite sizes in the membranes were smaller than those in the Cit/HAp NPs alone.[25] It is suggested that the NP sizes that can easily penetrate and diffuse into the polymer mesh spaces (*i.e.*, free space) interact with HYA during the nanohybrid process. SEM images of the membrane surface morphologies suggested the inclusion of the Cit/HAp NPs, implying that the Cit/HAp NPs may influence the surface and internal states of the nanohybrid membranes (Fig. S3, ESI†). The EDS elemental mapping and XRF indicated the presence of Ca and P elements in all the membranes, which were homogeneously distributed (Fig. S3, ESI†). From XRF, the weight ratio of (Na+C)/(Ca+P) was 0.99 for Cit/HAp-HYA, 0.95 for Cit/HAp-HYA_Et and 0.88 for Cit/HAp-HYA_Wa, suggesting that the washing process caused the elution of HYA or desorption of Cit[37] to reduce the proportion of organic compounds. The Ca/P molar ratio was about 1.3 for all the membranes, indicating that the Cit/HAp NPs were in the Ca-deficient apatite state.[38] Therefore, it was suggested that the hybridized organic compounds were desorbed and eluted to simultaneously abstract the Ca ion from the Cit/HAp NPs by the washing process.

AFM topographic and phase-shift images of the membranes are shown in Fig. 2. The topographic image of the Cit/HAp-HYA revealed the significant particulate structures with the root mean square roughness (R_{rms}) value of 12.6 nm. From the phase-shift image, rigid NPs were predominantly present on the membrane surfaces. Thus, the NPs that could not enter into the free spaces confined by the polymer chains were segregated on the membrane surfaces, when the polymers and NPs interacted in the solution. The topographic image of Cit/HAp-HYA_Et clearly shows the polymer microfibril structures with the R_{rms} value of 29.5 nm. The segregation of the much smaller

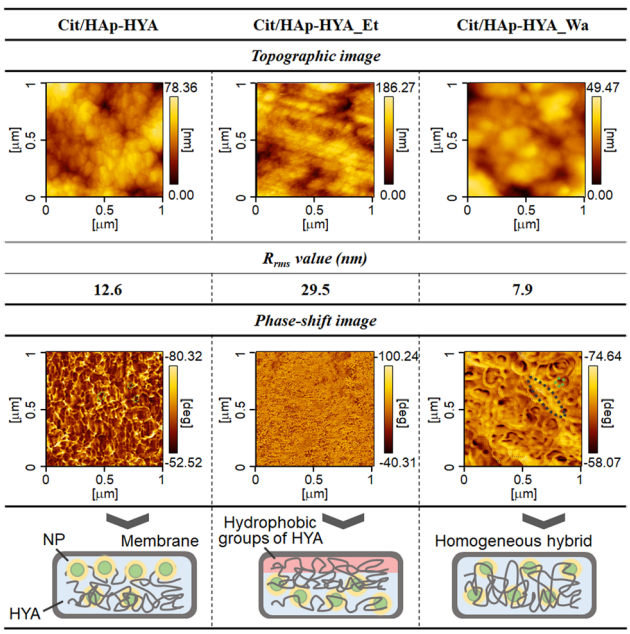

Fig. 2 AFM topographic and phase-shift images of the membranes, showing their R_{rms} values and the illustration of the hybridization states.

substances was also observed, which could be attributed to the precipitation and segregation of the nanocrystals (*e.g.*, calcium citrate hydrate, *etc.*).[39] The homogeneous phase-shift images indicated that the membrane surfaces were predominantly soft (*e.g.*, polymeric) surfaces. During ethanol washing, the Cit/HAp NPs would be washed away, and the hydrophobic interactions between HYA molecules were enhanced to cause aggregation near the membrane surfaces.[40] In Cit/HAp-HYA_Wa, the topographic image showed particulate structures with the R_{rms} value of 7.9 nm. The phase-shift image indicated the presence of both NPs and polymers and the hybridization homogeneously occurred. By the water-washing process, the swelling of HYA caused the rearrangement of the NPs to form homogeneous nanohybrid states.

The different nanostructures of the membranes could be attributed to the interactions at the inorganic–organic interfaces. Thus, the chemical bonding states were analyzed by FT-IR spectroscopy (Fig. S4, ESI†). HYA-Na exhibited the absorption bands of amide I (1653 cm^{-1}), C═O stretching vibration (1623 cm^{-1}), amide II (1563 cm^{-1}), C–O stretching vibration (1415 cm^{-1}), amide III (1379 cm^{-1}), C–O–C stretching vibration (1153 cm^{-1}) and C–OH stretching vibration (1022 cm^{-1}) of the characteristic HYA structures, respectively.[41,42] In the Cit/HAp NPs, the COO^- symmetric stretching vibration (1585 cm^{-1}) and COO^- asymmetric stretching vibration (1415 cm^{-1}) were attributed to Cit, and the P–O stretching vibration (1042 cm^{-1}) of HAp was additionally observed.[43,44] The characteristic absorption bands of HYA-Na and Cit/HAp NPs were observed in all the membranes, suggesting the hybridization. In particular, the amide I band is thought to be the reaction site of the HYA molecule,[23] and all the membranes showed red-shifts as compared with the case in HYA-Na, and 1641 cm^{-1} for HYA, 1645 cm^{-1} for Cit/HAp-HYA, 1644 cm^{-1} for Cit/HAp-HYA_Et, and 1640 cm^{-1} for Cit/HAp-HYA_Wa were observed (Fig. 3(a)). It was suggested that hydrogen bonding interactions among the –CONH groups (HYA-Na) or between the –CONH group (HYA-Na) and the $–COO^-$ group (Cit/HAp NPs) were formed. Accordingly, the interactions not only between the HYA chains but also between the chains and the Cit/HAp NPs would cause membrane formation and hybridization (Fig. 3(c) red-color square). On the O–H absorption bands related with the hydroxy groups of –CH–OH directly present in the polysaccharide of HYA-Na and water molecules, the curve fitting and peak separation results of the six components are shown in Fig. S5, ESI.† The characteristic absorption bands of the –CH–OH stretching vibrations of the HYA-Na and HYA were blue-shifted by the introduction of the Cit/HAp NPs (Fig. 3(c) blue-color speech bubble). In the –CH–OH groups in the HYA molecules, strong associations based on the intra- and intermolecular hydrogen bonding interactions are effectively formed, so that it is difficult to contribute to the blue-shift based on the bonding with the other functional groups in the membrane formation.

Focusing on the $–CH_3OH$ group, the introduction of NPs changed the hydration states around the $–CH_3OH$ group of HYA, and reduced the hydrogen bonding properties.[45] By comparing the relative proportions of the hydration layer

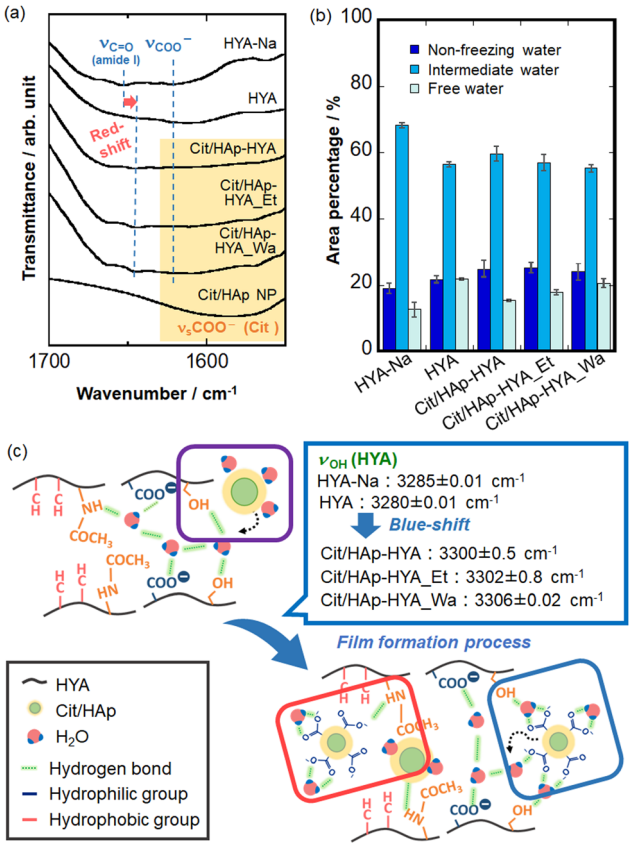

Fig. 3 FT-IR spectra of the membranes with the washing in the measurement region between (a) 1700–1500 cm^{-1}, (b) is the peak separation results in the region between 3800–2400 cm^{-1} to show the area percentages, and (c) is the illustration of the interfacial bonding formation process between the HYA and NPs based on the blue-shift of ν_{OH} of the end OH group in HYA.

through the curve fitting and peak separation results, it was observed that the hydration layer of the HYA tended to decrease the proportion of the intermediate water molecules and increase that of the free water and nonfreezing water molecules, as compared to the case in HYA-Na. In HYA-Na, the intermediate water molecules would cause relatively strong interactions between the HYA chains and water molecules to be retained between the HYA chains during the membrane formation process.[45] Furthermore, the proportion of nonfreezing water molecules increased slightly with the introduction of NPs (Fig. 3(b)), which could be attributed to the coordination of hydrated molecules of Cit with Ca ions of the NPs, [39] suggesting the successful introduction of NPs into the membranes (Fig. 3(c) purple-color square). From the TG-DTA analysis, the weight loss of the hydration layer can be calculated from the extrapolated ending temperature. Fig. S6, ESI† shows the weight losses of 6.5 wt% (Cit/HAp-HYA), 4.1 wt% (Cit/HAp-HYA_Et), and 6.5 wt% (Cit/HAp-HYA_Wa), respectively, indicating that the dehydration with ethanol reduced the hydration content. Furthermore, the curve fitting and peak separation results for the membranes that were left and exposed to air for an extended period (*ca.* five months) by the ATR method (Fig. S7, ESI†) increased the proportions of the free and intermediate water molecules in the hydration layer on the membrane surfaces, as compared to the case in the transmittance measurement. This was attributed to the absorption of more water molecules from the atmosphere on the surface of the membrane. Inside the membrane, the Cit-Ca hydrates[39] including the rigid nonfreezing water molecules were stabilized through the introduction of NPs, suggesting the interactions between the $-CH_3OH$ groups and NPs *via* the water in the membranes (Fig. 3(c) blue-color square). Therefore, the nanohybridization between Cit/HAp NPs and HYA molecules was mainly attributed to the hydrogen bonds formed between the –CONH and $-CH_3OH$ groups of the HYA molecules and the $-COO^-$ groups at the end of the NPs. Furthermore, the introduction and mediation of the water molecules of the Cit/HAp NPs significantly changed the hydration layer states of the membranes. We successfully prepared a film molding of the hybrid membrane. In particular, HYA has widely been used to take advantage of its biological properties.[46] Since the HYA surfaces interact with the cell surface receptors such as CD44,[47] our nanohybrid membranes are expected to be applied for cell culture substrates and regenerative-assisted materials.

Conclusions

We successfully realized the film molding of a hybrid membrane using the nanospace (*i.e.*, free space) and functional groups of HYA at the nanoscales. We found that the Cit/HAp NPs spontaneously interacted with the HYA molecules, causing the successful formation of self-standing and highly transparent nanohybrid membranes. Chemical interactions (*i.e.*, new hydrogen bonds) between the Cit/HAp NPs and HYA were found to form the membranes, leading to a change in the hydration states, which would be the strong interaction of Cit with water molecules. Our nanohybrid membranes will be applied for cell culture substrates and regenerative-assisted materials.

Author contributions

Conceptualization, A. E. and M. T.; methodology, A. E., Z. L. and M. M.; software, D. N.; validation, A. E. and M. T.; formal analysis, A. E.; investigation, A. E. and D. N.; resources, M. T.; data curation, A. E. and M. M.; writing – original draft preparation, A. E. and M. T.; writing – review and editing, Z. L., D. N. and M. M.; supervision, M. T.; project administration, M. T. All authors have read and agreed to the published version of the manuscript.

Conflicts of interest

There are no conflicts to declare.

Acknowledgements

This study was partially supported by a grant from the Japan Society for the Promotion of Science (JSPS) KAKENHI (Grant-in-

Aid for Challenging Exploratory Research, Grant 22K18916). The authors also thank the Analysis and Instrumentation Center at Nagaoka University of Technology for providing facilities. The authors thank Mr Masataka Saito, Ms Yanni Zhou, and Mr Syoma Hatori for their advice on the experimental analysis.

References

1 M. J. Olszta, X. Cheng, S. S. Jee, R. Kumar, Y. Y. Kim, M. J. Kaufman, E. P. Douglas and L. B. Gower, *Mater. Sci. Eng., R*, 2007, **58**, 77–116.
2 S. Weiner and W. Traub, *FASEB J.*, 1992, **6**, 879–885.
3 M. Tagaya, *Polym. J.*, 2015, **47**, 599–608.
4 J. Xie, M. J. Baumann and L. R. Mccabe, *J. Biomed. Mater. Res. A*, 2004, **71A**, 108–117.
5 Y. Chai, Z. Liu, D. Noda and M. Tagaya, *Solid State Phenom.*, 2021, **324**, 166–172.
6 C. M. Serre, M. Papillard, P. Chavassieux and G. Boivin, *Biomaterials*, 1993, **14**, 97–106.
7 T. Nishimura, H. Imai, Y. Oaki, T. Sakamoto and T. Kato, *Chem. Lett.*, 2011, **40**, 458–460.
8 T. Miyazaki, C. Ohtsuki, Y. Akioka, M. Tanihara, J. Nakao, Y. Sakaguchi and S. Konagaya, *J. Mater. Sci.: Mater. Med.*, 2003, **14**, 569–574.
9 M. Tanahashi, T. Yao, T. Kokubo, M. Minoda, T. Miyamoto, T. Nakamura and T. Yamamuro, *J. Appl. Biomat.*, 1994, **5**, 339–347.
10 T. Yokoi, M. Kawashita and C. Ohtsuki, *J. Asian Ceram. Soc.*, 2013, **1**, 155–162.
11 Y. Chai, M. Okuda, Y. Otsuka, K. Ohnuma and M. Tagaya, *Adv. Powder Technol.*, 2019, **30**, 1419–1423.
12 S. Sivasankari, R. Kalaivizhi, N. Gowriboy, M. R. Ganesh and M. Shazia Anjum, *Polym. Compos.*, 2021, **42**, 5512–5526.
13 C. Deng, J. Weng, X. Lu, S. B. Zhou, J. X. Wan, S. X. Qu, B. Feng and X. H. Li, *Mater. Sci. Eng., C*, 2008, **28**, 1304–1310.
14 M. Kikuchi, H. N. Matsumoto, T. Yamada, Y. Koyama, K. Takakuda and J. Tanaka, *Biomaterials*, 2004, **25**, 63–69.
15 F. J. Martínez-Vázquez, M. V. Cabañas, J. L. Paris, D. Lozano and M. Vallet-Regí, *Acta Biomater.*, 2015, **15**, 200–209.
16 S. S. Lee, M. Santschi and S. J. Ferguson, *Biomacromolecules*, 2021, **22**, 2460–2471.
17 Y.-H. Liang, C.-H. Liu, S.-H. Liao, Y.-Y. Lin, H.-W. Tang, S.-Y. Liu, I.-R. Lai and K. C.-W. Wu, *ACS Appl. Mater. Interfaces*, 2012, **4**, 6720–6727.
18 C.-Y. Chen, C.-J. Ke, K.-C. Yen, H.-C. Hsieh, J.-S. Sun and F.-H. Lin, *Theranostics*, 2015, **5**, 643–655.
19 T. Matsuda, H. Miwa, M. J. Moghaddam and F. Iida, *ASAIO J.*, 1993, **39**, M327–M331.
20 J. Y. Lee and A. P. Spicer, *Curr. Opin. Cell Biol.*, 2000, **12**, 581–586.
21 M. B. Asparuhova, V. Chappuis, A. Stähli, D. Buser and A. Sculean, *Clin. Oral Invest.*, 2020, **24**, 3923–3937.
22 J. E. Scott, *Ciba Found. Symp.*, 1989, **143**, 6–20.
23 K. Wada, *Sen'i Gakkaishi*, 2009, **65**, 407–411.
24 Z. Zhu, Y.-M. Wang, J. Yang and X.-S. Luo, *Plast. Aesthetic Res.*, 2017, **4**, 219.
25 S. C. De Smedt, A. Lauwers, J. Demeester, Y. Engelborghs, G. De Mey and M. Du, *Macromolecules*, 1994, **27**, 141–146.
26 I. Roohani, S. Cheong and A. Wang, *Open Ceram.*, 2021, **6**, 100092.
27 S. H. Jeong, Y. H. Koh, S. W. Kim, J. U. Park, H. E. Kim and J. Song, *Biomacromolecules*, 2016, **17**, 841–851.
28 X. Ma, L. Ma, Y. Tan, X. Chen, Q. Tong, L. Tang, X. Cao, D. Liu and X. Li, *Carbohydr. Polym.*, 2023, **322**, 121345.
29 J. H. Choi, S. O. Kim, E. Linardy, E. C. Dreaden, V. P. Zhdanov, P. T. Hammond and N. J. Cho, *J. Colloid Interface Sci.*, 2015, **448**, 197–207.
30 I. Gatej, M. Popa and M. Rinaudo, *Biomacromolecules*, 2005, **6**, 61–67.
31 T. Luan, L. Wu, H. Zhang and Y. Wang, *Carbohydr. Polym.*, 2012, **87**, 2076–2085.
32 G. Giubertoni, F. Burla, C. Martinez-Torres, B. Dutta, G. Pletikapic, E. Pelan, Y. L. A. Rezus, G. H. Koenderink and H. J. Bakker, *J. Phys. Chem. B*, 2019, **123**, 3043–3049.
33 Z. Liu, T. Kataoka, S. Samitsu, D. Kawagoe and M. Tagaya, *J. Mater. Chem. B*, 2022, **10**, 396–405.
34 Z. Liu, T. Kataoka, D. Kawagoe, D. Noda, Y. Chai and M. Tagaya, *Colloid Interface Sci. Commun.*, 2020, **39**, 100316.
35 R. G. Bates and G. D. Pinching, *J. Am. Chem. Soc.*, 1949, **71**, 1274–1283.
36 S. Kim, H.-S. Ryu, H. Suk Jung and K. Sun Hong, *Met. Mater. Int.*, 2004, **10**, 171–175.
37 T. Kataoka, T. Hashimoto, W. Shi and M. Tagaya, *Ind. Eng. Chem. Res.*, 2022, **61**, 10915–10921.
38 A. S. Posner, *Physiol. Rev.*, 1969, **49**, 760–792.
39 X.-C. Liu and L. H. Skibsted, *Int. Dairy J.*, 2022, **139**, 105561.
40 P. Matteini, L. Dei, E. Carretti, N. Volpi, A. Goti and R. Pini, *Biomacromolecules*, 2009, **10**, 1516–1522.
41 K. Haxaire, Y. Maréchal, M. Milas and M. Rinaudo, *Biopolymers*, 2003, **72**, 10–20.
42 R. Gilli, M. Kacuráková, M. Mathlouthi, L. Navarini and S. Paoletti, *Carbohydr. Res.*, 1994, **263**, 315–326.
43 M. A. Martins, C. Santos, M. M. Almeida, M. Elisabete and V. Costa, *J. Colloid Interface Sci.*, 2008, **318**, 210–216.
44 C. Li, *Mater. Res. Bull.*, 2009, **44**, 1136–1141.
45 N. Jouon, M. Rinaudo, M. Milas and J. Desbrihes, *Carbohydr. Polym.*, 1995, **26**, 69–73.
46 B. Kaczmarek, A. Sionkowska and A. M. Osyczka, *Polym. Test.*, 2017, **62**, 171–176.
47 K. Y. Choi, G. Saravanakumar, J. H. Park and K. Park, *Colloids Surf., B*, 2012, **99**, 82–94.